Electronic Supplementary Material (ESI) for Materials Chemistry Frontiers.

Electronic Supplementary Information

Designed Synthesis of Organosilica Nanoparticles for Enzymatic Biodiesel Production

Mohammad Kalantari, Meihua Yu,* Manasi Jambhrunkar, Yang Liu, Yannan Yang, Xiaodan Huang, and Chengzhong Yu*

Australian Institute of Bioengineering and Nanotechnology, The University of Queensland, Brisbane, QLD 4072, Australia.

E-mail: m.yu2@uq.edu.au; c.yu@uq.edu.au

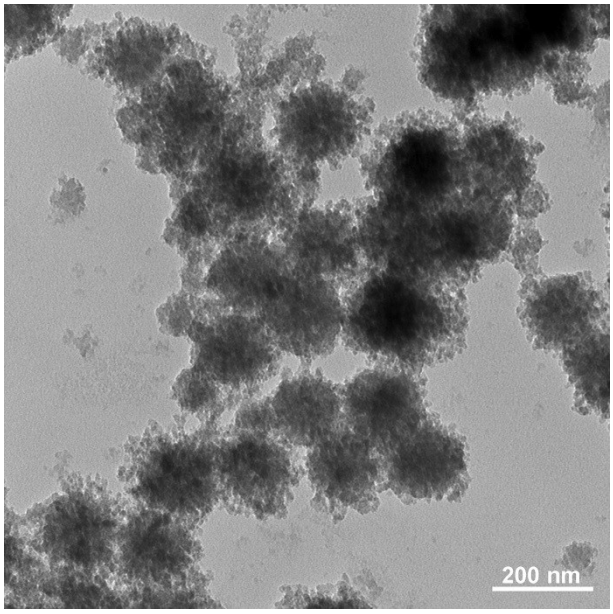

Fig. S1 TEM image of the BDMONs-15-1.5.

As shown in TEM image (Fig.S1), by further increasing the molar ratio of BTEB to TEOS to 1.5, the final product shows a non-porous structure with irregular morphology. This observation is consistent with previous reports in which the mesoporosity was substantially lost at high organosilanes to TEOS ratios.[1]

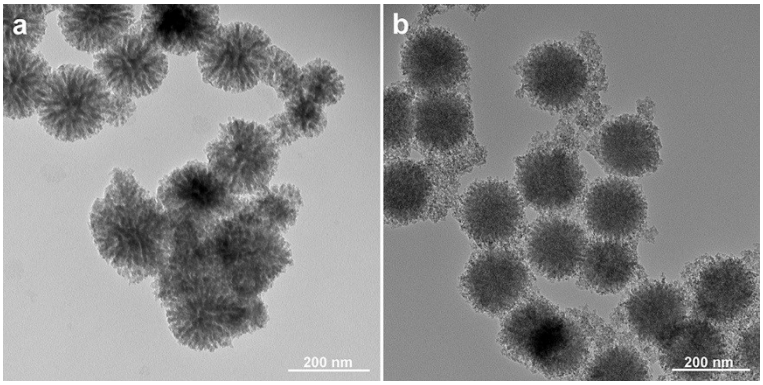

Fig. S2 TEM images of (a) BDMONs-5-0.5 and (b) BDMONs-30-0.5.

The time gap is a key parameter to obtain dispersed particle with the well-defined dendritic structure. As displayed by TEM images, under shorter and longer time gaps of 5 (Fig. S2a) and 30 (Fig.S2b) min, respectively, the obtained samples possess aggregated nanoparticles with ill-defined structure.

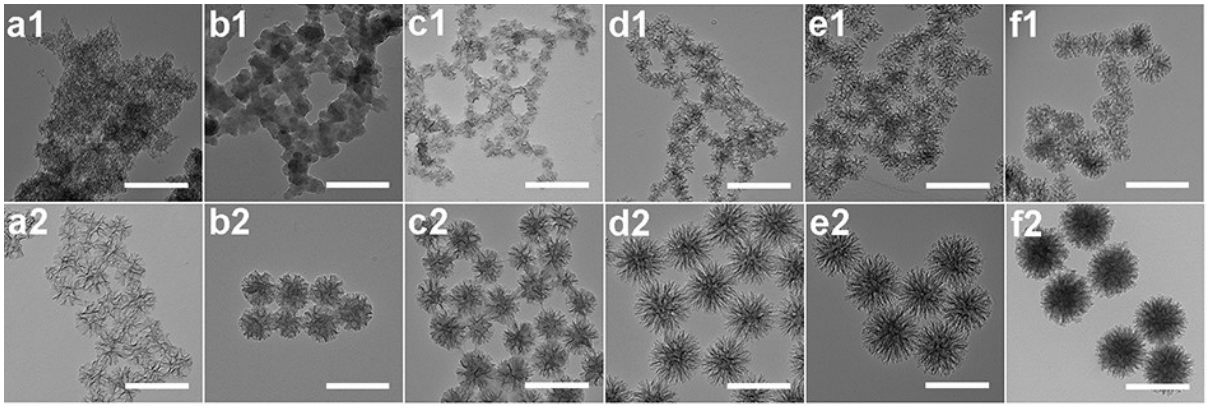

Fig. S3 TEM images of the samples obtained at the reaction time of 15 min (a1, a2), 30 min (b1, b2), 60 min (c1, c2), 3 h (d1, d2), 6 h (e1, e2), and 18 h (f1, f2) under the conditions for synthesis of BDMONs-0-0.5 (a1-f1) and BDMONs-15-0.5 (a2-f2). Scale bar is 200 nm.

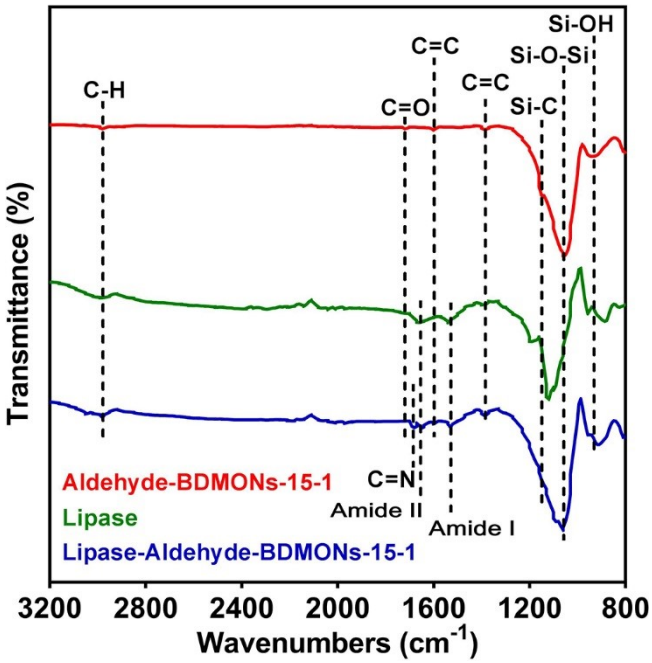

Fig. S4 FTIR spectra of Aldehyde-BDMONs-15-1, pure lipase, and Lipase-Aldehyde-BDMONs-15-1.

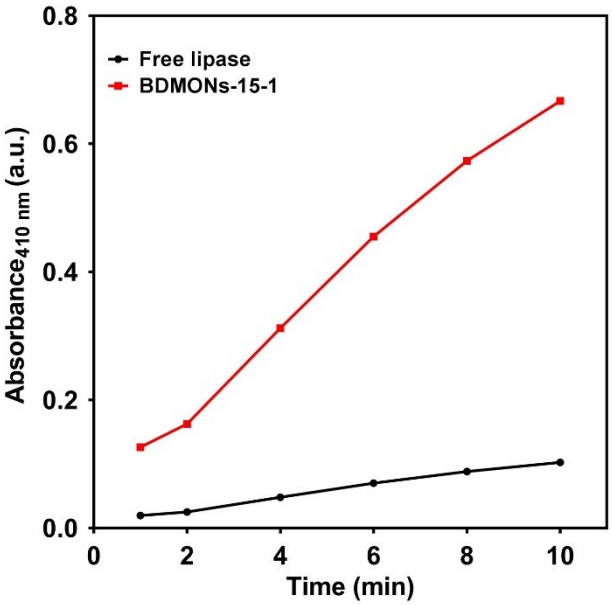

Fig. S5 Selected absorbance at 410 nm as a function of time for free lipase and BDMONs-15-1.

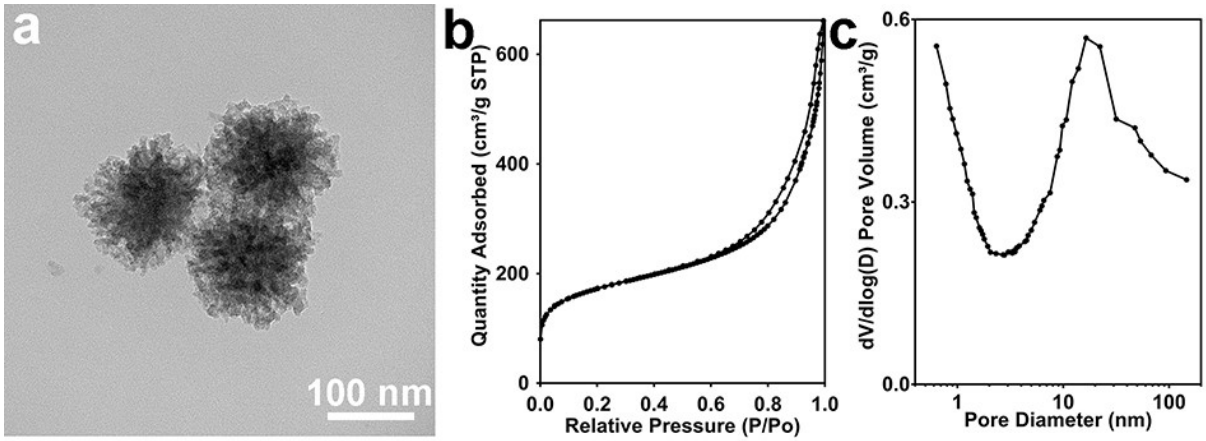

Fig. S6 (a) TEM image, (b) N_2 sorption isotherm and (c) pore size distribution curve of DMSNs.

As displayed by TEM image, DMSNs hold central-radial mesopore channels, similar to BDMONs-15-1 with a small reduction in particle size to 165 nm, attributing to silica framework shrinkage during high temperature calcination process (Fig. S6a and Table 1). The calcined sample also possesses type IV nitrogen sorption isotherm (Fig. S6b) with slightly enlarged pore diameter (16.5 nm, Fig. S6c) compared to BDMONs-15-1 (Table 1), indicating the success of organic groups removal.

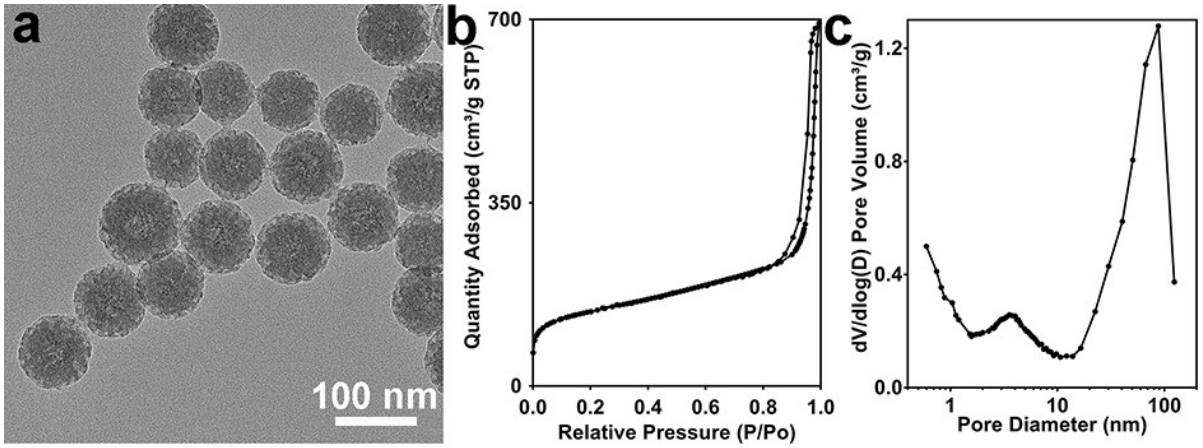

Fig. S7 (a) TEM image, (b) N_2 sorption isotherm and (c) pore size distribution curve of BONs-SP.

TEM image reveals that BON-SP possess a spherical morphology, small mesopore structure (2-3 nm) and a uniform diameter of 76 nm (Fig. S7a), smaller than BDMONs-15-1. BONs-SP exhibits type IV nitrogen sorption isotherm (Fig. S7b) and the corresponding pore size distribution curve (Fig. S7c) displays two peaks centred at 3.6 nm and 88 nm, contributed by the inner mesopores and voids generated by small particle aggregation, respectively. The surface area and pore volume of BONs-SP is 478 $m^2 g^{-1}$ and 1.092 $cm^3 g^{-1}$, respectively.

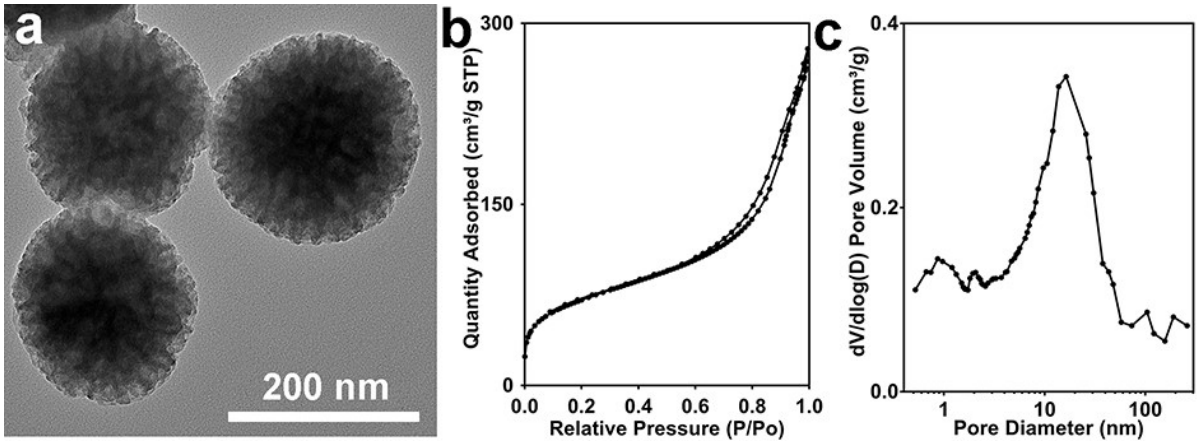

Fig. S8 (a) TEM image, (b) N_2 sorption isotherm and (c) pore size distribution curve of EDMONs-15-1.

As demonstrated by TEM image (Fig. S8a), EDMONs-15-1 show spherical morphology with a dendritic structure and an average particle size of 201 nm. EDMONs-15-1 displays type IV nitrogen sorption isotherms (Fig. S8b) with the pore diameter, surface area, and pore volume of 16.4 nm (Fig. S8c), 249 $m^2 g^{-1}$, and 0.436 $cm^3 g^{-1}$, respectively.

Table S1. Detailed synthesis parameters for nanoparticles.

Samples	Organosilica precursor	Time gap (min)	(Organosilica precursor/TEOS) molar ratio	NaSal (mg)
BDMONs-15-0.5	BTEB	15	0.5	42
BDMONs-15-0.67	BTEB	15	0.67	42
BDMONs-15-1	BTEB	15	1	42
BDMONs-15-1.5	BTEB	15	1.5	42
BDMONs-5-1	BTEB	5	1	42
BDMONs-30-1	BTEB	30	1	42
BDMONs-0-0.5	BTEB	0	0.5	42
BONs-SP	BTEB	15	1	0
EDMONs-15-1	BTEE	15	1	84

Table S2. Comparison of the catalytic performance of lipase immobilized on various carriers.

Carrier	Relative activity	Activity retention	Ref.
Meso-Structured Onion-Like Silica	0.35	NA	[2]
Magnetite nanoparticles	0.96	90% activity retained after five cycles	[3]
Magnetic silica particles	0.87	80% activity retained after five cycles	[4]
Olive pomace	0.90	91.7% activity retained after five cycles	[5]
Mesoporous silica particles	2.81	84% activity retained after five cycles	[6]
Nanoflowers	4.6	92% activity retained after eight cycles	[7]
Graphene oxide	1.3	NA	[8]
Graphene oxide	1.9	70% activity retained after eight cycles	[9]
Carbon dots	3.7	NA	[10]
Silica foam	1.23	NA	[11]
Mesoporous silica nanoparticles	5.23	93% activity retained after five cycles	[12]
PMO	2.02	NA	[13]
PMO	5.0	85% activity retained after four cycles	[14]
Magnetic nanoparticles	<1	NA	[15]
Gold/silica nanocomposite	0.67	NA	[16]
Magnetic silica particles	0.22	40% activity retained after thirty cycles	[17]
Magnetic carbon particles	0.93	68% activity retained after ten cycles	[18]
Macroporous silica	<1	NA	[19]
Graphene oxide	0.98	NA	[20]
Magnetic silica particles	0.89	89% activity retained after five cycles	[21]
Dopamine-functionalized meso-Structured Onion-Like Silica	0.52	71% activity retained after six cycles	[22]
BDMONs nanoparticles	6.5	99% activity retained after five cycles	This work

References

1. F. Hoffmann, M. Cornelius, J. Morell and M. Fröba, *Angew. Chem., Int. Ed.*, 2006, **45**, 3216-3251.
2. S.-H. Jun, J. Lee, B. C. Kim, J. E. Lee, J. Joo, H. Park, J. H. Lee, S.-M. Lee, D. Lee, S. Kim, Y.-M. Koo, C. H. Shin, S. W. Kim, T. Hyeon and J. Kim, *Chem. Mater.*, 2012, **24**, 924-929.
3. D. Jung, M. Paradiso, D. Wallacher, A. Brandt and M. Hartmann, *ChemSusChem*, 2009, **2**, 161-164.
4. M. Kalantari, M. Kazemeini and A. Arpanaei, *Biochem. Eng. J.*, 2013, **79**, 267-273.
5. Y. Yücel, *Bioresour. Technol.*, 2011, **102**, 3977-3980.
6. J. Liu, S. Bai, Q. Jin, H. Zhong, C. Li and Q. Yang, *Langmuir*, 2012, **28**, 9788-9796.
7. J. Cui, Y. Zhao, R. Liu, C. Zhong and S. Jia, *Sci. Rep.*, 2016, **6**, 27928.
8. M. Mathesh, B. Luan, T. O. Akanbi, J. K. Weber, J. Liu, C. J. Barrow, R. Zhou and W. Yang, *ACS Catal.*, 2016, **6**, 4760-4768.
9. A. Rezaei, O. Akhavan, E. Hashemi and M. Shamsara, *Chem. Mater.*, 2016, **28**, 3004-3016.
10. S. Sarkar, K. Das and P. K. Das, *Langmuir*, 2016, **32**, 3890-3900.
11. Q. Jin, G. Jia, Y. Zhang, Q. Yang and C. Li, *Langmuir*, 2011, **27**, 12016-12024.
12. M. Kalantari, M. Yu, Y. Yang, E. Strounina, Z. Gu, X. Huang, J. Zhang, H. Song and C. Yu, *Nano Res.*, 2017, **10**, 605-617.
13. E. Serra, E. Díez, I. Díaz and R. M. Blanco, *Microporous Mesoporous Mater.*, 2010, **132**, 487-493.
14. Z. Zhou, R. N. K. Taylor, S. Kullmann, H. Bao and M. Hartmann, *Adv. Mater.*, 2011, **23**, 2627-2632.
15. A. Dyal, K. Loos, M. Noto, S. W. Chang, C. Spagnoli, K. V. P. M. Shafi, A. Ulman, M. Cowman and R. A. Gross, *J. Am. Chem. Soc.*, 2003, **125**, 1684-1685.
16. U. Drechsler, N. O. Fischer, B. L. Frankamp and V. M. Rotello, *Adv. Mater.*, 2004, **16**, 271-274.
17. J. Lee, Y. Lee, J. K. Youn, H. B. Na, T. Yu, H. Kim, S.-M. Lee, Y.-M. Koo, J. H. Kwak, H. G. Park, H. N. Chang, M. Hwang, J.-G. Park, J. Kim and T. Hyeon, *Small*, 2008, **4**, 143-152.
18. Z. Chen, W. Xu, L. Jin, J. Zha, T. Tao, Y. Lin and Z. Wang, *J. Mater. Chem. A*, 2014, **2**, 18339-18344.
19. Y. Jiang, L. Shi, Y. Huang, J. Gao, X. Zhang and L. Zhou, *ACS Appl. Mater. Interfaces* 2014, **6**, 2622-2628.
20. S. Hermanova, M. Zarevucka, D. Bousa, M. Pumera and Z. Sofer, *Nanoscale*, 2015, **7**, 5852-5858.
21. P. Esmaeilnejad-Ahranjani, M. Kazemeini, G. Singh and A. Arpanaei, *Langmuir*, 2016, **32**, 3242-3252.
22. J. Gao, Y. Jiang, J. Lu, Z. Han, J. Deng and Y. Chen, *Sci. Rep.*, 2017, **7**, 40395.